Received: 7 December 2020 | Revised: 10 March 2021 | Accepted: 11 March 2021

DOI: 10.1002/fam.2967

RESEARCH ARTICLE

WILEY

The combustion behavior of epoxy-based multifunctional electrolytes

Natasha Shirshova[1] | Thomas Rogaume[2] | Hussain Najmi[2] | Marc Poisson[2]

[1]Department of Engineering, Durham University, Durham, UK

[2]Institut Pprime, CNRS, Departement Fluides, Thermique, Combustion, Université de Poitiers, ENSMA, Futuroscope Chasseneuil Cedex, France

Correspondence
Natasha Shirshova, Department of Engineering, Durham University, South Road, Durham, DH1 3LE, UK.
Email: natasha.shirshova@durham.ac.uk

Funding information
Engineering and Physical Sciences Research Council, Grant/Award Numbers: EP/P007546/1, EP/T013044/1; French Government programme 'Investissements d'Avenir', Grant/Award Number: LABEX INTERACTIFS reference ANR-11-LABX-0017-01

Summary

Multifunctional or structural electrolytes are characterized by ionic conductivity high enough to be used in the electrochemical devices and mechanical performance suitable for the structural applications. Preliminary insights are provided into the combustion behavior of structural bi-continuous electrolytes based on bisphenol A diglycidyl ether (DGEBA), synthesized using the techniques of reaction induced phase separation and emulsion templating. The effect of the composition of the structural electrolytes and external heat flux on the behavior of the formulations were studied using a cone calorimeter with gases formed during testing analyzed using FTIR. The composition of the formulations investigated was changed by varying the type and amount of the ion conductive part of the bi-continuous electrolyte. Two ionic liquids, 1-ethyl-3-methylimidazolium bis(fluorosulfonyl)imide (EMIM-TFSI) and 1-butyl-3-methylimidazolium tetrafluoroborate (BMIM-BF_4), as well as a deep eutectic solvent (DES) based on ethylene glycol and choline chloride, were used. The results obtained confirm that time to ignition, heat release rate (HRR), total mass loss, as well as the composition of the gases released during tests depend on the composition of the formulations. Addition of liquid electrolyte is found to reduce the time to ignition by up to 10% and the burning time by between 28% and 60% with the added benefit of reducing the HRR by at least 34%. Gaseous products such as CO_2, CO, H_2O, CH_4, C_2H_2, N_2O, NO, and HCN were detected for all formulations with the gases SO_2, NH_3, HCl, C_2H_4, and NH_3 found to be for certain formulations only.

KEYWORDS
bicontinuous structures, combustion behavior, epoxy resin, gaseous emissions, ionic liquid, multifunctional electrolytes, thermal decomposition, time to ignition

1 | INTRODUCTION

Multifunctional energy storage devices can simultaneously perform two functions: combining a structural role with an electrical storage capability, which provides volume and weight savings, and makes them especially attractive for applications in areas such as portable electronics, aircraft, and electrical or hybrid vehicles.[1-2] Research into multifunctional energy storage devices is focused on three principal types: batteries, capacitors, and supercapacitors,[1,3-4] examples for all main types of energy storage mechanisms. Here, the focus is structural supercapacitors since, apart from exhibiting fast charge-discharge, their architecture resembles that of laminated composite materials. In addition, both composites and supercapacitors benefit from the presence of carbon and a polymer: carbon is used as an electrode material in energy storage devices and as a reinforcement in composites, while a polymer can form part of the electrolyte in

supercapacitors and a matrix in composites. To date, the majority of the effort has been directed at improving the performance of individual components and the overall mechanical and electrochemical performance of structural energy storage devices.[1,5-8] However, as the technological advances in multifunctional energy storage devices in general and more specifically structural supercapacitors matures, a focus on mechanical properties and electrochemical performance alone is insufficient, as additional questions arise which require answering. One such question concerns the fire safety of these devices and their constituents.

It is difficult to overestimate the safety issues surrounding energy storage devices, especially after the number of related fire accidents that have been reported,[9] mainly caused by thermal runaway of batteries. Not surprisingly, the latter has led to a significant amount of published research concerning batteries, directed at understanding the mechanism of thermal runaway, batteries' performance when exposed to fire, the influence of their individual components, and their fire dynamics.[9-17] Indeed, the majority of work on the fire safety of energy storage devices has been directed at batteries, most likely as they represent the main large scale commercially used type of energy storage device. It has been reported that lithium-ion batteries generate significant amounts of heat, with total heat release (THR) values strongly dependent on the state of the charge of the battery.[10,14,17] However, high temperature and the amount of heat released are not the only reported danger associated with lithium-ion batteries under fire conditions; the toxic gases emitted during the fire is another key factor which cannot be overlooked.[14] Such gases include not only CO_2 and H_2O but also flammable and toxic ones, that is, CH_4, CO, and HCl,[17-18] where the flammable hydrocarbons being products of the decomposition of the electrolyte and separator present in the battery.[18] Research into the fire safety of energy storage devices includes studies of the individual components,[16,18-19] full lithium-ion batteries, and battery packs.[14-15,17]

There is also a significant number of reports on the fire properties of fiber-reinforced composites, from both an experimental and modeling perspective.[20-27] Interest in studying the behavior of fiber-reinforced composite materials exposed to the fire is due to their wide range of applications, from sports equipment and medical prosthetics, to ships and aircraft, as well as less usual applications such as unmanned aerial vehicles (UAVs), space launchers, and satellites.[28] Often, composite materials are used to replace metal, since composites provide a combination of high mechanical performance, lightweight, and a resistance to corrosion. However, unlike metals and alloys, when subjected to fire, composite materials can produce volatile gases and vapors, both flammable (CO, CH_4, etc) and nonflammable (CO_2, H_2O, etc), together with fumes and smoke.[29] The production of flammables gases can lead to increased heat, assisting in the growth and spread of fire, while toxic gases and smoke can result in reduced visibility and pose a serious hazard to both the environment and human health. The literature shows that tests have been performed under various conditions with the help of number of instruments, from tubular furnaces to cone calorimeter[24,30] apparatus, looking at mass loss, the kinetic mechanisms of thermal decomposition, heat release rate (HRR), and the release gases from the oxidation.[22,24,31] In most cases, the matrix is the main source of volatile products which could reduce the HRR due to the endothermic nature of the decomposition reactions of the organic materials. However, the composition of the volatile products emitted during thermal decomposition depends on the nature of the matrix and the heating process, as well as the atmosphere. A wide range of matrices are used in fiber-reinforced composite materials with epoxy being one of the most widely studied. To improve their fire performance, the effect of number of factors has been investigated, from the type of curing agent used[32] to the presence and type of fire retardants.[33]

However, structural electrolyte contains not only epoxy resin but also a liquid electrolyte,[7,34-38] with bicontinuous epoxy-based electrolytes containing ionic liquid (IL) and deep eutectic solvent (DES) showing great potential for application in structural supercapacitors, as they exhibit a good balance of mechanical performance and ionic conductivity.[7,34-36] ILs are salts with a melting temperature below room temperature and a unique combination of properties — such as high ionic conductivity, low vapor pressure, a wide voltage window, as well as their safety aspects when compared to organic electrolytes. Due to the potential of the ILs for various applications including energy storage, the question of their safety has received a lot of attention.[39-42] It has been shown[39,42] that despite ILs being difficult to ignite their associated HRR can be as high as 8000 kW/m^2, with the HRR and toxicity of the emission produced depending significantly on the composition of the IL.[42]

Despite the interest shown in the fire safety of structural energy storage devices, to the best of our knowledge, there is no information regarding the fire/combustion properties of their individual components or of devices as a whole reported in the literature. Moreover, there is no information available concerning the fire/combustion properties of epoxy-IL blends. The purpose of the work reported here is to address this omission in the literature. Here, we present data concerning the fire properties of structural electrolytes comprising of epoxy resin and IL/DES, determined using a cone calorimeter and two heat fluxes, 35 and 50 kW/m^2. The effect of composition on the ignition time, HRR, mass loss, and the gases emitted are presented and discussed.

2 | MATERIALS AND METHODS

2.1 | Materials

Bisphenol A diglycidyl ether (DGEBA), hardener isophorone diamine (iPDA), choline chloride (ChCl, ≥98.0%) and ethylene glycol (EG, 99.8%) were purchased from Sigma Aldrich. ILs: 1-ethyl-3-methylimidazolium bis(fluorosulfonyl)imide (EMIM-TFSI, >99%), 1-butyl-3-methylimidazolium tetrafluoroborate (BMIM-BF_4, 99%) were purchased from Ionic Liquid Technologies. The surfactant Cithrol DPHS-SO-(MV) (Cithrol) was kindly provided by Croda. All chemicals were used as received.

2.2 | DES preparation

The DES was synthesized by mixing ChCl and EG in 1:3M ratio[43] at 80°C and constant stirring using a magnetic stirrer for 24 hours. The

ionic conductivity of synthesized DES was determined to be 7.58 mS/cm which is in agreement with data reported in the literature.[43]

2.3 | Preparation of the structural electrolytes

2.3.1 | Synthesis of structural electrolytes via reaction induced phase separation

DGEBA was dissolved in the required amount of IL followed by the addition of the measured amount of iPDA. Next, the mixture was stirred until a homogeneous solution was obtained following degassing. Prepared formulations were cured using horizontal silicon moulds to produce plaques with dimensions 100 mm × 100 mm and thickness of 3 to 4 mm. For curing the following cycle was used:

1. dwell at room temperature for 22 hours;
2. ramp to 60°C at 2°/min; dwell at 60°C for 1 hour;
3. ramp to 80°C at 2°/min; dwell at 80°C for 2 hours.

Samples were cooled down to the room temperature, removed from the moulds and post cured using the following cycle:

1. ramp to 120°C at 6°C min^{-1};
2. hold at 120°C for 2 hours.

Samples were cooled in the oven to a room temperature prior to their removal from the oven.

2.3.2 | Structural electrolyte using medium internal phase emulsion approach

Medium internal phase emulsions (MIPEs) were prepared using a glass reaction vessel equipped with a glass paddle rod connected to an overhead stirrer. The continuous phase was prepared by dissolving surfactant in the hardener and after a solution was formed the epoxy was added, ensuring the weight ratio of DGEBA to iPDA was 1:4. The mixture was stirred using the overhead stirrer until a solution was obtained. Internal phase (DES; 50 vol%) was added dropwise under continuous stirring at 500 rpm. After all the internal phase was added, the stirring rate was increased to 2000 rpm for 2 minutes to further homogenize the emulsion. The prepared emulsions were transferred into the horizontal silicon mould as above to obtain plaques with the same dimensions. The MIPEs were polymerized using the curing cycle described in the previous section.

The structures of the all main compounds and compositions used for synthesis of the formulations studied are presented in Figure 1 and Table 1, respectively.

2.4 | Cone calorimeter test

The thermal decomposition and the combustion behavior of the different formulations were studied in a cone calorimeter,[44] manufactured by Fire Testing Technology Limited, under well-ventilated conditions. Tests were carried out with a piloted ignition (spark ignition plug) positioned above the sample surface in an air atmosphere (atmospheric conditions) and were repeated at least three times for

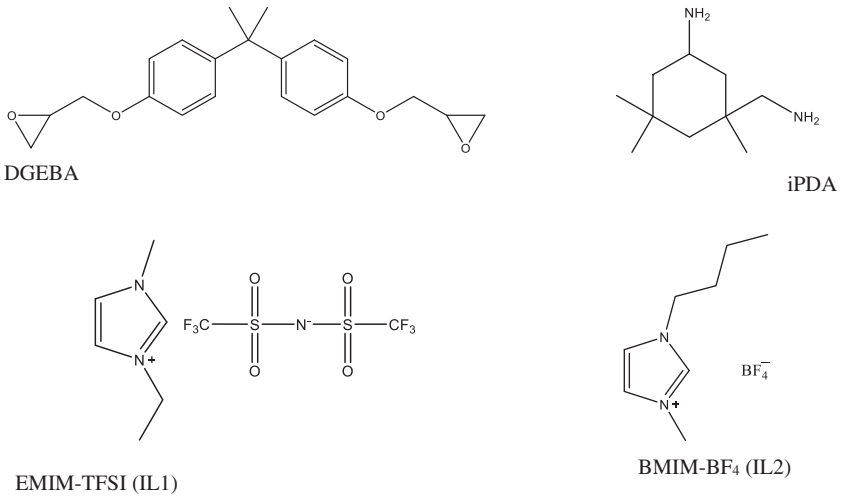

FIGURE 1 The structures of compounds used for synthesis of the formulations studied

TABLE 1 The compositions of the formulations studied

Sample	DGEBA (g)	iPDA (g)	EMIM-TFSI		$BMIM\text{-}BF_4$		DES	
			vol%	(g)	vol%	(g)	vol%	(g)
DGEBA	35.50	8.88	-	-	-	-	-	-
60DGEBAIL1	21.30	5.33	40	24.48	-	-	-	-
65DGEBAIL1	23.08	5.77	35	21.42	-	-	-	-
65DGEBAIL2	23.08	5.77	-	-	35	16.94	-	-
polyMIPE[a]	10	2.47	-	-	-	-	50	26.9

Note: The DGEBA:iPDA molar ratio was kept at 2:1 for all formulations.
Abbreviations: $BMIM\text{-}BF_4$, 1-butyl-3-methylimidazolium tetrafluoroborate; DES, deep eutectic solvent; EMIM-TFSI, 1-ethyl-3-methylimidazolium bis(fluorosulfonyl)imide.
[a]2.18 g of surfactant was also added to this formulation.

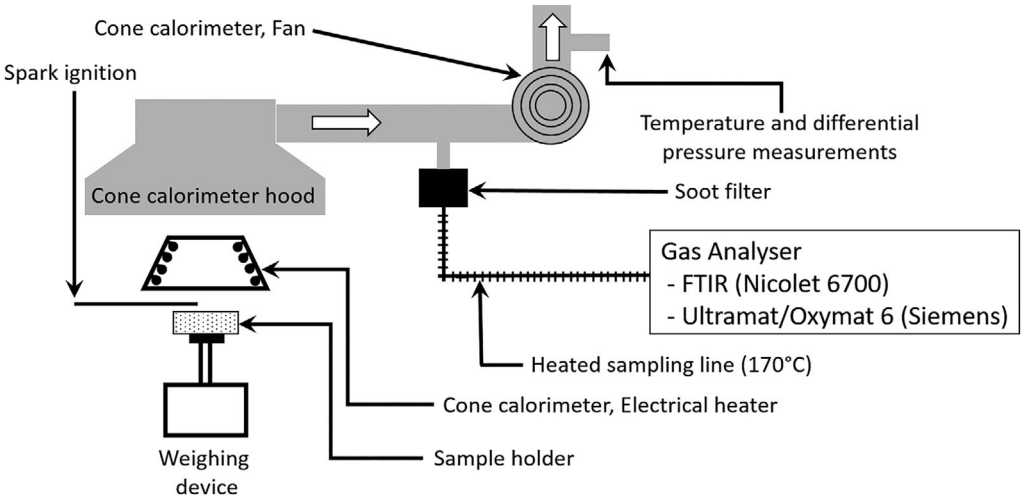

FIGURE 2 Schematic layout of the ISO 5660 cone calorimeter used

each formulation to ensure experimental reproducibility. Two heat fluxes 35 and 50 kW/m^2 were used.

Samples were placed on a standard cone metal holder, orientated horizontally, on a 4 cm bed of glass wool with a density of 90 kg/m^3, which insulated the back side of the specimen to minimize the heat loss effects. Furthermore, an aluminum foil was wrapped around the edges and the back of sample to prevent dripping. All of this conforms to the ISO 5660 standard.[44] During the experiment, mass loss, mass loss rates (MLR), and piloted ignition time were recorded simultaneously. The details of the apparatus, instrumentation, and standard test procedure for the cone calorimeter can be found in ISO 5660-1:2002.[44]

A Thermo-Nicolet 6700 Fourier Transformed Infrared (FTIR) spectrometer (mid-infrared spectrum with wave numbers between 750 and 4000 cm^{-1}, apodization = Happ-Genzell, number of scan = 1 corresponding to one spectrum every; 4 seconds, resolution = 0.5 cm^{-1} and data spacing; 0.25 cm^{-1}) equipped with an MCT-A detector (cooled by liquid nitrogen) and a measurement gas cell (T = 165°C, volume = 0.2 L and optical path-length = 2 m) to allow for the identification and quantification of gaseous species concentrations (in many cases, the relative uncertainty was estimated to be in the range 5%-10%). The gas sampling flow rate, obtained from an aspiration/suction pump that pulls the gas from the cone calorimeter sampling ring up to the FTIR spectrometer (Figure 2), is controlled by a float flowmeter and fixed at 2.0 NL min^{-1}.[45-46] Moreover, the sampling pressure was fixed at a constant value regulated by a control valve at 650 Torrs.[45-46] The FTIR analyser was calibrated beforehand using a single pure gas to N_2 standards with well-known concentration to quantify 15 gaseous combustion products (CO, CO_2, NO, NO_2, SO_2, NH_3, HCN, N_2O, CH_4, C_2H_2, C_2H_4, C_2H_6, C_3H_6, C_3H_8, and HCl) and H_2O (manual calibration at ambient temperature and pressure) at different concentrations (ca. 20 for each species except H_2O) during the experiments and to account for any interference between species.

The FTIR analysis technique used has been validated during the SAFIR project[45-46] which constituted the basis for fire gases analysis carried out following the guidelines of the standard ISO 19702.[47-53]

3 | RESULTS AND DISCUSSION

Four structural electrolytes were chosen for this study based on their performance, that is, ionic conductivity and mechanical properties, which were analyzed and discussed in details

TABLE 2 Properties of the formulations studied

Sample	Electrolyte	Ionic conductivity (mS/cm)	Young's Modulus (GPa)	Type of mechanical testing	Source
DGEBA (EP)	-	-	3.03	3 point bending	36
60DGEBAIL_1	EMIM-TFSI	1.81	0.29	3 point bending	36
65DGEBAIL_1	EMIM-TFSI	0.28	0.80	3 point bending	36
65DGEBAIL_2	BMIM-BF_4	1.17	0.50	3 point bending	54
polyMIPE	DES	1.90	0.21	Compression	35

Abbreviations: BMIM-BF_4, 1-butyl-3-methylimidazolium tetrafluoroborate; DES, deep eutectic solvent; EMIM-TFSI, 1-ethyl-3-methylimidazolium bis(fluorosulfonyl)imide.

TABLE 3 Effect of composition on properties of epoxy based formulations

	Time to ignition [a] (s)		Flame time (s)		pHRR (kW/m^2)		THR (MJ/m^2)		weight remaining (wt%)		
Sample	35 kW/m^2	50 kW/m^2	35 kW/m^2	50 kW/m^2	35 kW/m^2	50 kW/m^2	35 kW/m^2	50 kW/m^2	35 kW/m^2	50 kW/m^2	Density (g/cm^3)
DGEBA	222 ± 11	170 ± 8	504 + 236	316 ± 134	1327 ± 60	1603 ± 108	108 ± 12	113 ± 2	4.8 ± 3.0	2.8 ± 1.7	1.040 ± 0.090
60DGEBA_IL1	203 ± 6	156 ± 2	219 ± 34	195 ± 21	782 ± 124	1040 ± 81	59 ± 6	67 ± 2	20.9 ± 2.4	18.9 ± 8.6	1.270 ± 0.035
65DGEBA_IL1	201 ± 7	162 ± 1	249 ± 37	222 ± 63	822 ± 58	1056 ± 135	72 ± 9	69 ± 9	19.5 ± 7.2	16.9 ± 9.2	1.270 ± 0.025
65DGEBA_IL2	206 ± 5	168 ± 5	394 ± 61	336 ± 37	656 ± 12	1037 ± 43	97 ± 3	101 ± 4	13.5 + 2.7	8.5 ± 3.7	1.140 ± 0.040
polyMIPE	173	n.t.	414	n.t.	612	n.t.	129	n.t.	2	n.t.	n.t.

Abbreviations: n.t., not tested; pHRR, peak HRR; THR, total heat release.
[a]Time is not normalized for 125 seconds; external flux 35 kW/m^2; T = 540°C and external flux 50 kW/m^2; T = 668°C.

elsewhere.[35-36,54] The properties of the formulations studied are listed in Table 2.

3.1 | Effect of the composition on time to ignition, flame time, and mass loss rate

Time to ignition is one of the crucial parameters in the study of materials and devices as it shows how long a sample can be exposed to heat before it ignites and initiates a flame. It was observed that among formulations studied, neat epoxy (DGEBA) was the last to ignite for both of the heat fluxes considered (35 and 50 kW/m^2). However, neat DGEBA also burned the longest. It can be seen (Table 3) that even though IL containing structural electrolytes ignite faster, they also burn faster.

All the structural electrolytes studied have highly porous structure (Figure 3) which affects heat transfer through the structure. As the thermal conductivity of the IL is lower compared to that of epoxy,[55-58] heat transfer from the top epoxy face through the thickness of the bicontinuous structure of the structural electrolyte is lower compared to a sample of neat epoxy. Hence, the top surface of the structural electrolyte samples exposed to the cone heater is heated rapidly and ignites before the neat epoxy sample. The reduction in burning time with the addition of IL is probably due to the lower epoxy content in structural electrolytes, the high thermal stability of ILs,[42,59] and the bicontinuous nature of the structural electrolytes microstructure. The reduction in epoxy content also led to the increase in the remaining sample mass after the test (Table 3, Figure 4). This further confirms that the primary source of the ignition and thermal decomposition is the epoxy resin. Note that, it was impossible to weigh residuals after the test as char from the epoxy was dispersed in the thermally oxidized IL and spread over the sample holder (Figure S2).

It can also be seen from Table 3 that the peak heat release rate (pHRR), for both heat fluxes, is a function of epoxy content in the samples formulations studied, except for 65DGEBA_IL2 at 35 kW/m^2. The difference in the behavior observed for 65DGEBA_IL2 can be explained by the possible variations in the thicknesses of the samples and their microstructural anisotropy. Due to the poor overall performance, including fast time to ignition, high mass loss, and high THR, of the polyMIPE samples at 35 kW/m^2, it was decided not to test them at 50 kW/m^2.

In case of structural electrolytes studied, four processes take place during the test: (a) the emission of combustible gases; (b) ignition, when the concentration of the combustible gases is high enough; (c) burning of the structural electrolyte; and (d) extinguishing of the flames. As structural electrolytes consist of two separate phases (Figure 3),[36] the following is of note: when the solid epoxy phase burned out it released the liquid phase, initially confined in the pores, some of which seeped through the sample holder and some getting burned, exposing more of the solid epoxy phase with the cycle continuing until all epoxy resin is burned. A smaller loss of IL during the testing was observed for samples containing BMIM-BF_4 in comparison to EMIM-TFSI. The difference in performance of the

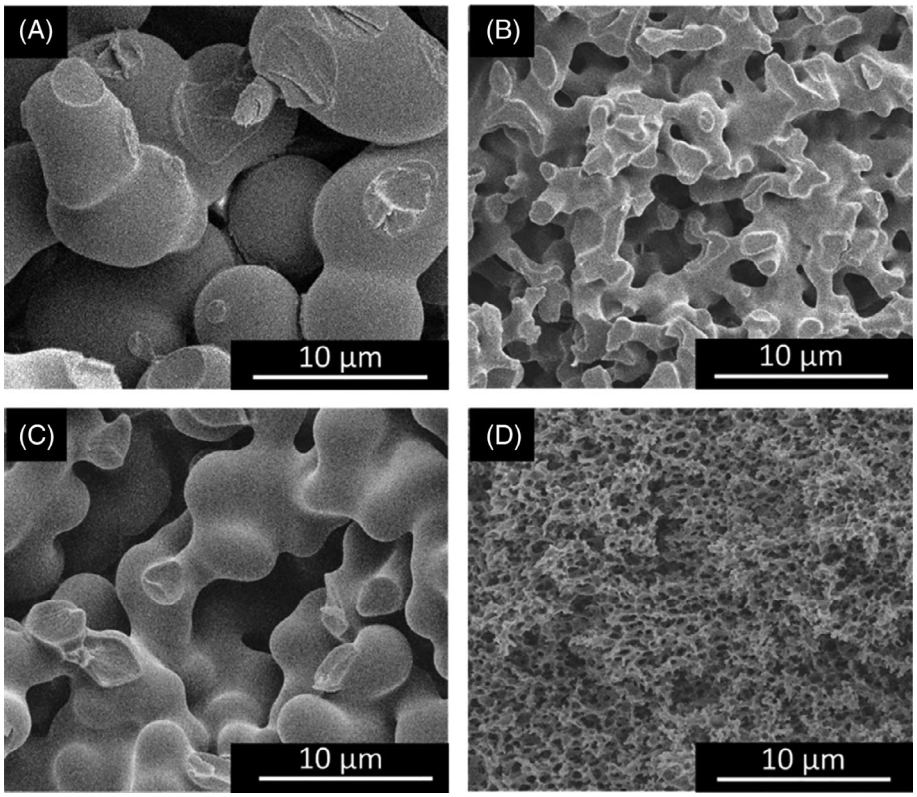

FIGURE 3 Representative SEM images for the studied formulations: A, 60DGEBAIL_1; B, 65DGEBAIL_1; C, 65DGEBAIL_2; and D, polyMIPE

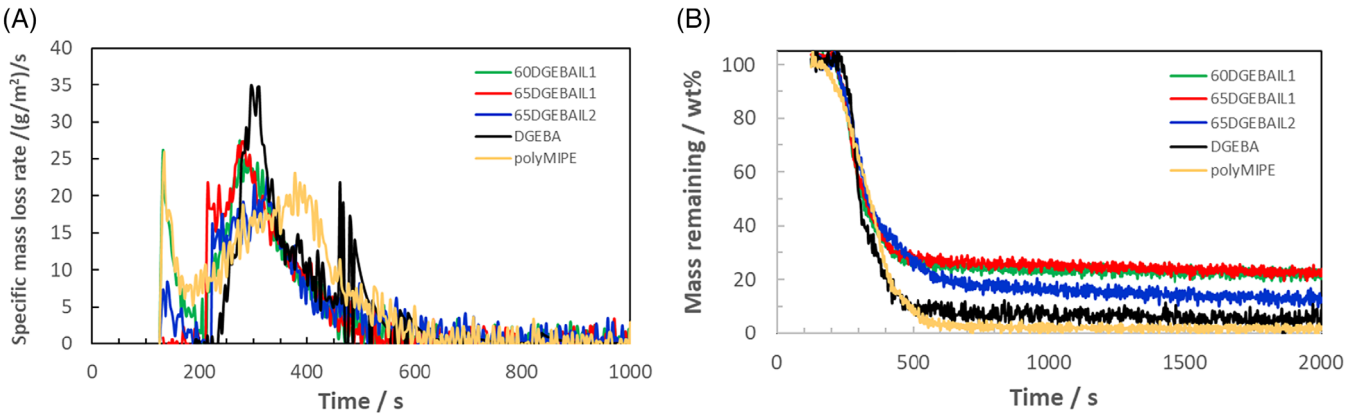

FIGURE 4 Effect of composition on (A) specific mass loss rate and (B) remaining mass, at an external heat flux of 35 kW/m^2

structural electrolytes containing different ILs could be due to the variation of the thermal stability of individual ILs. According to the literature, the onset of the decomposition temperature, determined via TGA, was 399°C and 419°C for BMIM-BF_4 and EMIM-TFSI, respectively.[41] Unexpectedly, this difference in onset decomposition temperature did not affect the ignition time of the structural electrolytes, as only a slight variation in its value was observed for 65DGEBAIL_1 and 65DGEBAIL_2 (Table 3). Note also that the heat capacity of EMIM-TFSI is higher than that of BMIM-BF_4,[60] which suggest that EMIM-TFSI could be responsible for reducing the local temperature, performing the role of a thermal barrier, and as a result increasing the amount of residual char (Table 3). Another reason for the observed differences in behavior of the formulations is their physical properties, more specifically their densities. The density of the neat epoxy was calculated to be roughly 1 g/cm^3 (Table 3), whether both ILs had densities >1 g/cm^3, and more specifically, 1.52 and 1.21 g/cm^3 for EMIM-TFSI and BMIM-BF_4, respectively. As a result the formulations containing EMIM-TFSI had a higher density compared to neat epoxy and structural electrolyte containing BMIM-BF_4 (Table 3). It has been reported[61] that the physical properties of polymers have a significant effect on polymer flammability and specifically that polymers with lower density will reach the critical pyrolysis flux before polymers with a higher density. Even

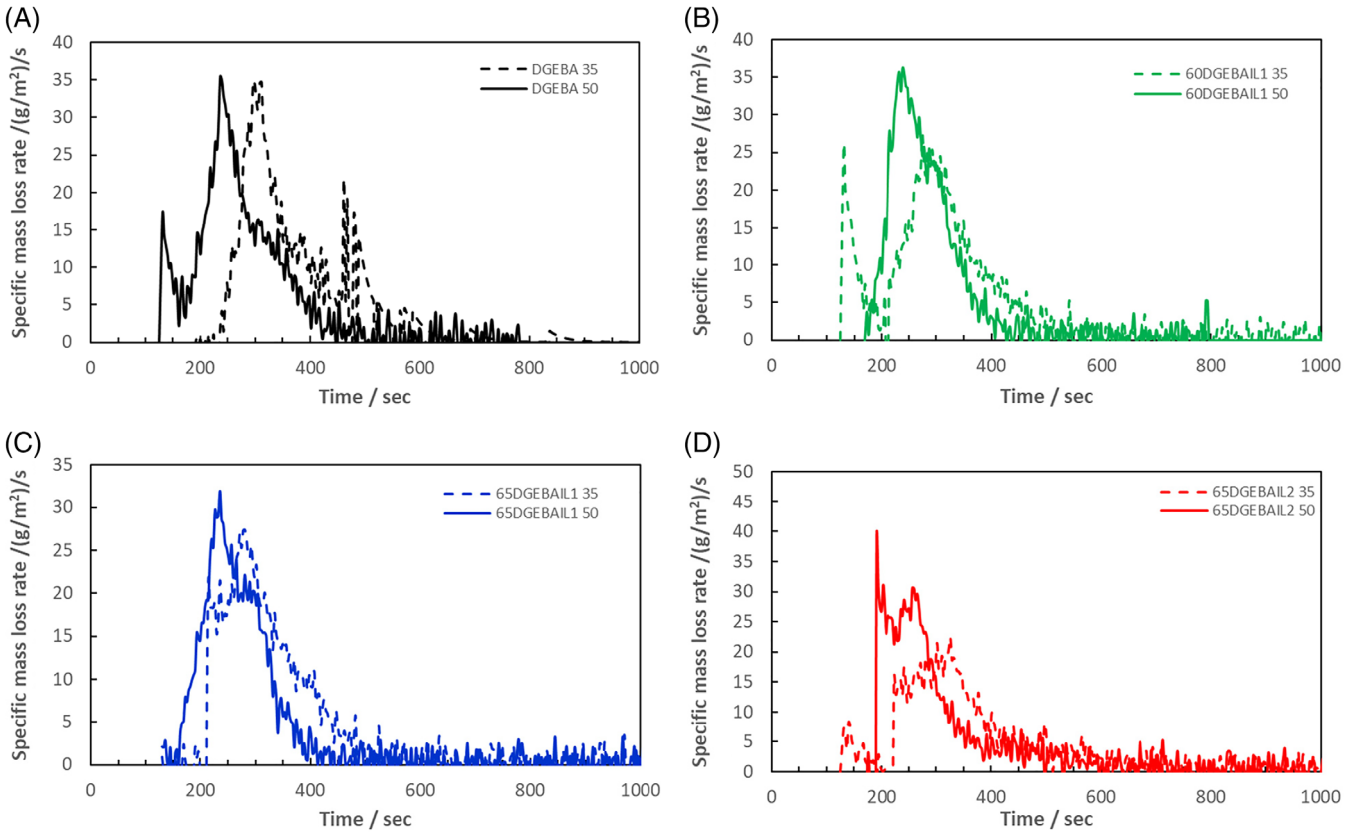

FIGURE 5 Specific mass loss rate for individual formulations at external heat fluxes 35 kW/m^2 (dashed line) and 50 kW/m^2 (solid line): A, DGEBA; B, 60DGEBA_IL1; C, 65DGEBA_IL1, and D, 65DGEBA_IL2

though this conclusion was made for the case of solid polymers, it is reasonable to assume that it is also valid for porous polymers.[61]

Figure 4 shows the effect of composition on the specific mass loss rate (SMLR) and the remaining weight of formulations studied. The SMLR curves for all of individual formulations studied can be found in Figure S2. It can be seen (Figure 4) that some of the formulations have a peak at an early stage of the experiment, which is most likely caused by the evaporation of the water absorbed by the ILs.[62] If present, the early peak is followed by the main peak, which for structural electrolyte containing BMIM-BF_4 is less sharp in comparison to other formulations (Figure 4A). However, the amplitude of the SMLR curves for all formulations is similar with the main stage of the thermal decomposition occurring between 200 and 600 seconds. Out of all of formulations studied, polyMIPE showed the lowest remaining weight of just 2 wt%, followed by the neat epoxy (4 wt%) and formulations containing ILs (Figure 4B, Table 3). The behavior observed for polyMIPE could be explained by the relatively earlier onset of thermal decomposition of the DES, which according to the literature is below 250°C.[63]

Changing the external heat flux from 35 to 50 kW/m^2 resulted in an increase of the maximum of the SMRL peaks for formulations containing ILs, with a minimal change in the shape of the peak (Figure 5). An increase in the heat flux also resulted in a reduction of the weight remaining after the test. For all formulations studied, thermal decomposition started earlier when the heat flux was increased to 50 kW/m^2. This suggests that the increased heat flux lowers the thermal resistance of the formulations, accelerating decomposition and increasing the release rate of volatile compounds. Structural electrolytes containing BMIM-BF_4 (65DGEBA_IL2) showed (Figure 5) a different decomposition profile compared to the rest of the formulations.

3.1.1 | Effect of composition on heat release rate and total heat release

Heat release rate (HRR) is one of the most important parameters in helping to characterize the combustion of the materials and to understand and quantify the hazards of unwanted fires[64] as it allows the rate of the fire growth and the amount of toxic gases generated to be calculated. HRR curves for all of formulations studied, see Figure 6, are estimated at a heat flux of 35 and 50 kW/m^2. It can be seen that the HRR depends strongly on the composition of the formulations (Figure 6, Table 3). As mentioned earlier, four processes can be observed during the testing, and subsequently, the HRR curve can be divided into four zones. The first is ignition, which is the part of the curve before the beginning of the peak (at around 200 seconds,

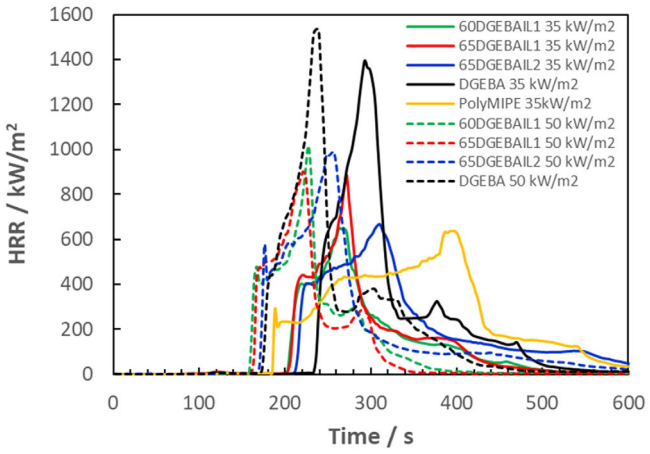

FIGURE 6 Effect of the composition on the heat release rate curves at 35 kW/m^2 (solid line) and 50 kW/m^2 (dashed line)

Figure 6); the second is fire development, which is represented by the beginning of the HRR peak; the third is pHRR, that is, the maximum of the HRR peak; the fourth is an extinction phase, the part of the curve following the pHRR. For all formulations, the initial delay (zone one) could be observed because the temperature on the surface did not reach the decomposition temperature. Depending on the formulation, the length of the zone 1 varies from 173 seconds for polyMIPE to 222 seconds for neat epoxy. Zone 1 is followed by the zone 2 and represented by an increase in HRR values as volatiles (mainly low-molecular-weight hydrocarbons) formed near the polymer/fire interface started to combust. This further suggests that the initial decomposition is due to the epoxy resin, as it has a lower decomposition temperature[66] in comparison to the ILs.[41] Moreover, for all formulations studied, zone 1 and 2 overlap with each other, showing that concentration and type of liquid electrolyte do not impact the initial decomposition process. It can be seen (Figure 6) that only the neat epoxy sample has a sharp peak and all other formulations having a sharp increase followed by the step increase in HRR values, most likely due to the difference in thermal stabilities of the structural part of the electrolyte, that is, the epoxy, and liquid electrolyte part, that is, ILs and DES. The step increase for formulations containing liquid electrolytes can be also explained as follows: after the initial delay stage and as soon as the concentration of the volatile gases are high enough, they combusted which results in an increase of the local temperature leading to the production of the more volatile gases. However, their amount is insufficient for continuous burning to occur, as the liquid electrolyte in the epoxy formulations could act as a cooling agent, reducing the temperature and, as a result, reducing the rate of heat release. As decomposition of the sample progresses and its amount reduces, the HRR starts to decrease with time until the decomposition is completed and the HRR value becomes negligible. The results presented shown that zones 1, 2, and 3 correspond mainly to the decomposition of the epoxy, which was also confirmed by the exhaust gas emission and is discussed in the next section; while zone 4 can be attributed to decomposition of the liquid electrolyte. It should also be noted that the HRR for neat epoxy is in a good agreement with data reported in the literature.[65] The pHRR in the case of 65DGEBA_IL 2 is slightly delayed, while for samples containing IL1, pHRR is observed with no obvious delay despite the variation in the epoxy resin content. The observed behavior is due to the difference in the thermal conductivity of the ILs (Table 4). The higher the thermal conductivity of the IL, the longer the delay in reaching the pHRR. It is reasonable to suggest that the pHRR value depends on the epoxy content, while the time to reach it depends on the thermal properties of the liquid electrolyte. This is the reason why, in the case of polyMIPE, zone 2 is stretched over a longer period compared to the other structures even though the epoxy content is the lowest among the formulations studied. With the heat flux is increased to 50 kW/m^2, the first zone showed very small variation for samples studied independent of their composition (Table 3 and Figure 6), suggesting that at the high heat flux, the presence of liquid electrolyte does not have a pronounced effect on the time to ignition.

TABLE 4 Thermal conductivity of different elements of studied formulations

Elements	Thermal conductivity (W/m·K)	References
Epoxy	0.25	[57]
EMIM-TFSI (IL1)	0.13-0.161	[55]
BMIF-BF_4 (IL2)	0.19	[56]
DES	0.245	[58]

Abbreviations: BMIM-BF_4, 1-butyl-3-methylimidazolium tetrafluoroborate; DES, deep eutectic solvent; EMIM-TFSI, 1-ethyl-3-methylimidazolium bis(fluorosulfonyl)imide.

Furthermore, an increase in the external heat flux from 35 to 50 kW/m^2 led to a significant rise in the HRR peak values, THR values, and a reduction of the initial delay stage of the process (Table 3, Figure 7). According to the literature, TFSI-anions oppose the heat release more strongly than BF_4 anions,[59] but this was concluded for ILs with the same cation. It is clear that the size of cation also affects the fire performance of ILs, and that in this study, the HRR peak for formulations containing BMIM-BF_4 is significantly lower in comparison to those with EMIM-TFSI. The effect of the contribution of cation and anion on the fire performance of IL was not the focus of this research and, without further investigation, it is difficult to arrive at a definite conclusion regarding the level of the influence of individual components in each formulation. The change in the external heat flux did not affected the general shape of the HRR curves, showing that even though the rate of the decomposition of the studied formulations increased, it did not affect the individual stages of the process.

The THR data (Figure 8) also confirm that the epoxy resin is responsible for the initial decomposition of the formulations studied containing liquid electrolytes, as the initial decomposition of all the formulations showed minimum variations irrespective of the IL used. In the later stage of the decomposition, that is, around 300 seconds into the beginning of the thermal decomposition (Figure 8), the THR also increased as the percentage of an ionic liquid (EMIM-TFSI) increased from 35% to 40%. The average increase in THR for 60DGEBA_IL1 after the point where the two curves (60DGEBA_IL1

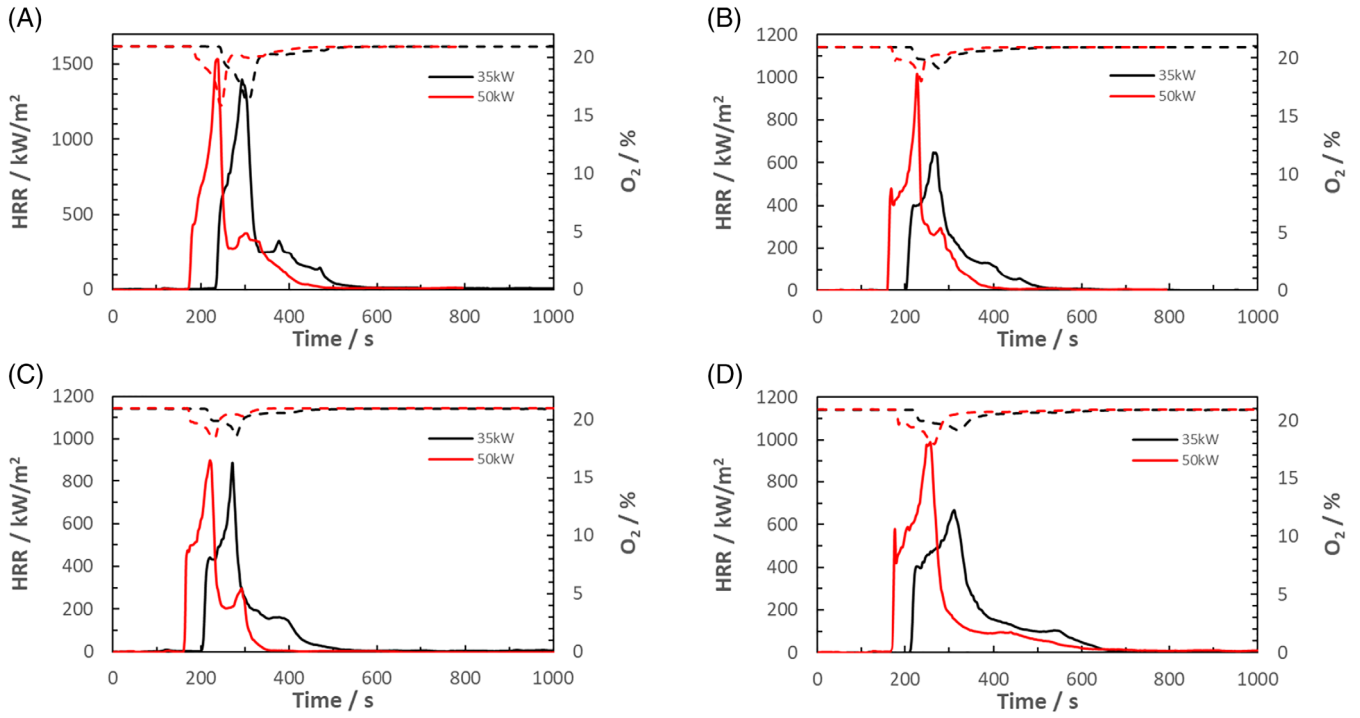

FIGURE 7 Effect of the external heat flux on the heat release rate of studied formulations with different composition; A, DGEBA; B, 60DGEBA_IL1; C, 65DGEBA_IL1; and D, 65DGEBA_IL2

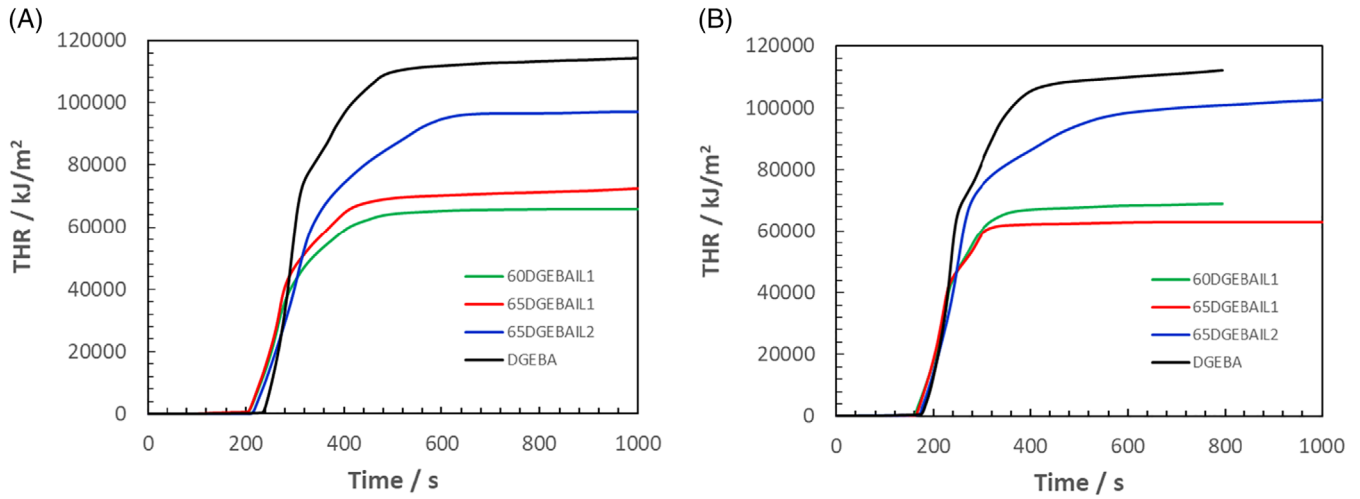

FIGURE 8 Total heat release of different formulations at, (A) 35 kW/m^2 and (B) 50 kW/m^2

and 65DGEBA_IL1) separate is about 7%, which is close to the difference in the amount of the *IL* present in the initial formulations. This also confirms that the behavior observed for the HRR curves at the stage of flame extinction conforms with the decomposition of the ILs. Figure 8 also confirms that the IL2 (BMIM-BF_4) contributes more to the thermal decomposition compared to IL1 (EMIM-TFSI) which means formulations containing IL1 are more stable compared to those containing IL2.

3.2 | Effect of the composition on gases released

One of the main causes of the death during accidental fires is the presence of toxic gases released during combustion processes, in which CO is the most important toxicant.[21,66] Evolution curves of the concentrations of CO, H_2O, NO, CH_4, SO_2, HCl, HCN, and NO_2 are plotted as functions of time for an external heat flux of 35 kW/m^2 (Figure 9). For all studied structural electrolytes, an increase in

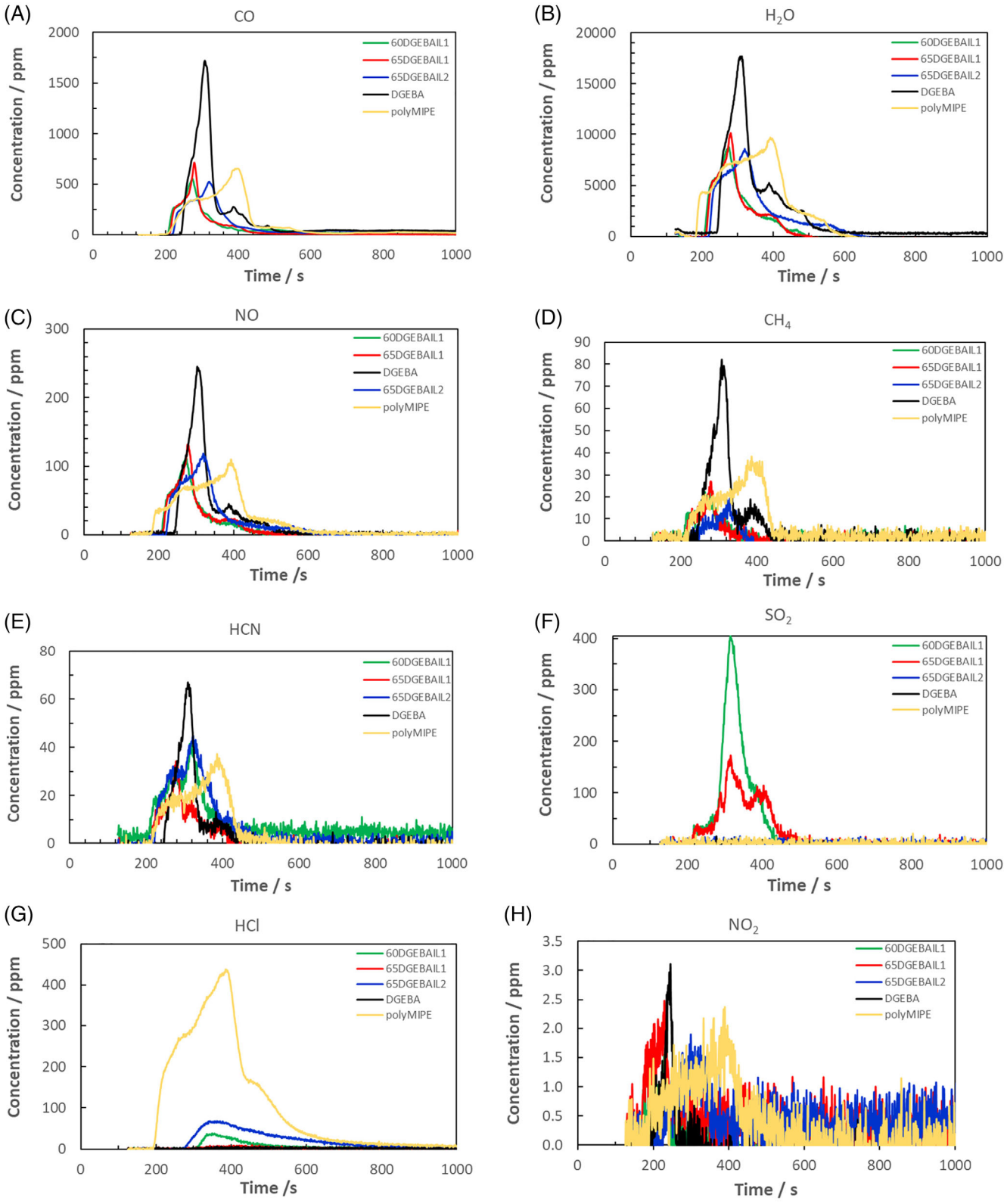

FIGURE 9 Evolution of the main exhaust gases in case of different structures at the heat flux of 35 kW/m^2

heat flux to 50 kW/m^2 resulted in an increase of pyrolysis rate and the production of combustible gases (graphs are not presented here).

It can be seen that the amount of the gaseous emissions depended strongly on the composition of the formulations studied. Introduction of liquid electrolyte leads to a significant reduction in the amount CO

released during tests (Figure 9), suggesting that the main contributor to the formation of CO is epoxy resin. This is in a good agreement with data available in the literature where it has been suggested that CO is a product of the first step of the pyrolysis reaction of the polymer ($\text{Polymer} + O_2 \xrightarrow{T} CO + H_2O + \text{Other products}$).[65-66] If enough oxygen is available, CO would slowly oxidase forming CO_2 ($CO + 0.5O_2 \rightarrow CO_2$). However, this process is limited to the amount of oxygen present, and the initial polymer pyrolysis stage could be faster than the following oxidation. For all formulations studied, the curves showing the formation of H_2O follow a similar pattern to CO which is expected.

The thermal decomposition of epoxy for a heat flux of 35 kW/m^2 resulted in the production of not only CO and CO_2 but a number of other gaseous products, such as CH_4, C_2H_4, NO, and so on. Significant amounts of CO (with the peak value of 1400-2000 ppm), C_2H_4 (25-30 ppm), and CH_4 (70-100 ppm) were detected during the HRR peak. The formulations containing IL1 and IL2 showed a decrease in the production of these gases compared to the neat epoxy. The gaseous product profile for polyMIPE differs slightly from the other formulations studied, since it not only produces CO (12 500 ppm) and CH_4 (650 ppm) (Figure 9) but also some C_3H_6 (190 ppm) and C_3H_8 (35 ppm) (graphs are not presented here) which were not detected for any of the other formulations. The reduction in the amount of gaseous products detected, for the structural electrolytes containing ILs, indicates that the presence of ILs results in a decrease in formation of toxic gases resulting in a safer material compared to a neat epoxy.

Detailed descriptions of the decomposition phases of the epoxy-based formulations, reported elsewhere,[21,30] indicate that the thermal decomposition of epoxy resin is characterized by random chain scission, end chain scission, and chain stripping reactions. The presence of the nitrogen in the formulations, both in iPDA and ILs, resulted in formation of NO and HCN. It should be noted that most of the NO and HCN formed is coming from the epoxy as indicated by a combination of following factors: the peaks for neat epoxy which were greater and the weight loss of the neat epoxy was greater than those of structural electrolytes. It was has also been reported,[10] that nitrogen oxide could be also produced as a reaction product of nitrogen (originating from air or fuel-bound N_2) and oxygen from air within the flame. The presence of SO_2 and HCl in emitted gaseous mixture, in the case of formulations containing IL1, is formed from the decomposition of the EMIM-TFSI.

4 | CONCLUSION

Potential applications of the multifunctional/structural supercapacitors range from the portable electronic devices to automotive and aerospace industry, and for all of them, safety is of the prime concerns. Multifunctional electrolyte is an essential part of the supercapacitor which plays a major role in combustion properties of the device as a whole. Initial studies of the fire/combustion properties of the neat epoxy and structural electrolytes based on epoxy resin have been performed using a cone calorimeter and applying two external heat fluxes, 35 and 50 kW/m^2. The effect of the composition and heat flux on the ignition time, mass loss rate, HRR, and THR were studied. The main gaseous emissions were characterized using an FTIR spectrometer. It was shown that even though structural electrolytes will catch fire faster, the amount of heat produced was over 50% less and the flame time was almost twice as fast as neat epoxy. The HRR results suggest the initial decomposition of formulations with IL is governed by epoxy content in the sample. This phenomenon was also confirmed by the THR results. The slight advancement in ignition time for the formulations with ILs was attributed to the lower thermal conductivity of IL in comparison to epoxy. pHRR values were also mainly affected by the amount of epoxy in the formulations, while time to reach them is mainly dependent on the thermal conductivity of the respective IL. The addition of the IL to the epoxy resin resulted in a decrease of the flame time and the production of toxic and combustible gases, which in combination with their ionic conductivity and mechanical performance reveal their great potential in real world applications. While PolyMIPE also showed great potential in terms of flame time and pHRR, consideration should be given to use of an alternative DES as an internal phase. This conclusion was made based on the fast ignition, high THR value, as well as increased formation of CO and CH_4 observed during the testing of the polyMIPE.

ACKNOWLEDGMENTS

Natasha Shirshova would like to acknowledge the EPSRC for their financial support through projects "Safety and Fire reaction of structural power storage devices" EP/T013044/1 and "Beyond structural: multifunctional composites that store electrical energy" EP/P007546/1. Natasha Shirshova also acknowledges help with SEM imaging provided by Dr W. Quan. This work pertains to the French Government programme "Investissements d'Avenir" (LABEX INTERACTIFS, reference ANR-11-LABX-0017-01). The authors are also immensely thankful to the "Institut des Risques Industriels Assurantiels et Financiers" of the University of Poitiers for the technical support it provided.

CONFLICT OF INTEREST

The authors declare there is no conflict of interest.

ORCID

Natasha Shirshova https://orcid.org/0000-0002-0546-6278
Hussain Najmi https://orcid.org/0000-0003-1478-2392

REFERENCES

1. Snyder JF, Gienger EB, Wetzel ED. Performance metrics for structural composites with electrochemical multifunctionality. *J Comp Mater*. 2015;49(15):1835-1848.
2. Carlstedt D, Asp LE. Performance analysis framework for structural battery composites in electric vehicles. *Composites Part B*. 2020;186:107822.
3. Carlson T, Asp LE. An experimental study into the effect of damage on the capacitance of structural composite capacitors. *J Multifunct Comp*. 2013;1(2):91-97.
4. Shirshova N, Qian H, Houllé M, et al. Multifunctional structural energy storage composite supercapacitors. *Faraday Discuss*. 2014;172:1-23.

5. Asp LE, Johansson M, Lindbergh G, Xu J, Zenkert D. Structural battery composites: a review. *Funct Compos Struct*. 2019;1:042001.
6. Qian H, Diao H, Shirshova N, et al. Activation of structural carbon fibres for potential applications in multifunctional structural supercapacitors. *J Colloid Interface Sci*. 2013;395:241-248.
7. Shirshova N, Bismarck A, Greenhalgh ES, et al. Composition as a control of morphology and properties of epoxy and ionic liquid based dual-phase structural electrolytes. *J Phys Chem C*. 2014;118:28377-28387.
8. Beringer IR, Walter M, Snyder JF, Wetzel ED. Multifunctional structural polymer electrolytes via interpenetrating truss structures. *Multifunct. Mater.* 2018;1:015005.
9. Sun P, Huang X, Bisschop R, Niu H. A review of battery fires in electric vehicles. *Fire Technol*. 2020;56:1361-1410.
10. Ribière P, Grugeon S, Morcrette M, Boyanov S, Laruellea S, Marlair G. Investigation on the fire-induced hazards of Li-ion battery cells by fire calorimetry. *Energ Environ Sci*. 2012;5:5271-5280.
11. Kong L, Li C, Jiang J, Pecht MG. Li-ion battery fire hazards and safety strategies. *Energies*. 2018;11:2191.
12. Liu X, Stoliarov SI, Denlinger M, Masias A, Snyder K. Comprehensive calorimetry of the thermally-induced failure of a lithium ion battery. *J Power Sources*. 2015;280:516-525.
13. Wang Q, Mao B, Stoliarov SI, Sun J. A review of lithium ion battery failure mechanisms and fire prevention strategies. *Prog Energy Combust Sci*. 2019;73:95-131.
14. Wang Z, Ouyang D, Chen M, Wang X, Zhang Z, Wang J. Fire behavior of lithium-ion battery with different states of charge induced by high incident heat fluxes. *J. Therm. Anal. Calorim.* 2019;136:2239-2247.
15. Peng Y, Zhou X, Hu Y, Ju X, Liao B, Yang L. A new exploration of the fire behaviors of large format lithium ion battery. *J. Therm. Anal. Calorim.* 2020;139:1243-1254.
16. Mei J, Liu H, Chen M. Experimental study on combustion behavior of mixed carbonate solvents and separator used in lithium-ion batteries. *J. Therm. Anal. Calorim.* 2020;139:1255-1264.
17. Zhong G, Mao B, Wang C, et al. Thermal runaway and fire behavior investigation of lithium ion batteries using modified cone calorimeter. *J Therm Anal Calorim*. 2019;135:2879-2889.
18. Eshetu GG, Grugeon S, Laruelle S, et al. In-depth safety-focused analysis of solvents used in electrolytes for large scale lithium ion batteries. *Phys Chem Chem Phys*. 2013;15:9145-9155.
19. Na R, Lu N, Zhang S, et al. Facile synthesis of a high-performance, fire-retardant organic gel polymer electrolyte for flexible solid-state supercapacitors. *Electrochim Acta*. 2018;290:262-272.
20. Brown JR, Mathys Z. Reinforcement and matrix effects on the combustion properties of glass reinforced polymer composites. *Comp Part A*. 1997;28A:675-681.
21. Mouritz AP, Gibson AG. *Fire Properties of Polymer Composite Materials*. Dordrecht, The Netherlands: Springer; 2006:416.
22. Mouritza AP, Mathys Z, Gibson AG. Heat release of polymer composites in fire. *Composites: Part A*. 2006;37:1040-1054.
23. Schuhler E, Coppalle A, Vieille B, Yon J, Carpier Y. Behaviour of aeronautical polymer composite to flame: a comparative study of thermoset- and thermoplastic-based laminate. *Polym. Degrad. Stabil.* 2018;152:105-115.
24. Hertzberg T. Dangers relating to fires in carbon-fibre based composite material. *Fire Mater*. 2005;29:231-248.
25. Fateh T, Zhang J, Delichatsios M, Rogaume T. Experimental investigation and numerical modelling of the fire performance for epoxy resin carbon fibre composites of variable thicknesses. *Fire Mater*. 2017;41:307-322.
26. Evegren F, Hertzberg T. Fire safety regulations and performance of fibre-reinforced polymer composite ship structures. *J Eng Maritime Environ*. 2017;231(1):46-56.
27. Mouritz AP, Feih S, Kandare E, et al. Review of fire structural modelling of polymer composites. *Composites: Part A*. 2009;40:1800-1814.
28. Soutis C. Fibre reinforced composites in aircraft construction. *Progr Aerospace Sci*. 2005;41:143-151.
29. Dao DQ, Rogaume T, Luche J, Richard F, Valencia LB, Ruban S. Thermal degradation of epoxy resin/carbon fiber composites: influence of carbon fiber fraction on the fire reaction properties and on the gaseous species release. *Fire Mater*. 2016;40:27-47.
30. Dao DQ, Luche J, Richard F, Rogaume T, Bourhy-Weber C, Ruban S. Determination of characteristic parameters for the thermal decomposition of epoxy resin/carbon fibre composites in cone calorimeter. *Int J Hydrogen Enrgy*. 2014;38:8167-8178.
31. Toldy A, Szolnoki B, Marosi G. Flame retardancy of fibre-reinforced epoxy resin composites for aerospace applications. *Polym Degrad Stabil*. 2011;96:371-376.
32. Ernault E, Richaud E, Fayolle B. Thermal oxidation of epoxies: influence of diamine hardener. *Polym. Degrad. Stabil.* 2016;134:76-86.
33. Jiao C, Zhang C, Dong J, Chen X, Qian Y, Li S. Combustion behavior and thermal pyrolysis kinetics of flame retardant epoxy composites based on organic–inorganic intumescent flame retardant. *J. Therm. Anal. Calorim.* 2015;119:1759-1767.
34. Shirshova N, Bismarck A, Carreyette S, et al. Structural supercapacitor electrolytes based on bicontinuous ionic liquid–epoxy resin systems. *J Mater Chem A*. 2013;1:15300-15309.
35. Clough B, Hollyman L, Quan W-D, Shirshova N. Polymerisied medium internal phase emulsions as structural separators. *ICCM22 2019*. Melbourne, VIC: Engineers Australia; 2019:4087-4094.
36. Wendong Q, Dent J, Arrighi V, Cavalcanti L, Shaffer MSP, Shirshova N. Structural electrolytes: Multifunctional block-copolymers as a way of properties modification. *Multifunc Mater*. 2020.
37. Yu Y, Zhang B, Wang Y, et al. Co-continuous structural electrolytes based on ionic liquid, epoxy resin and organoclay: effects of organoclay content. *Mater Des*. 2016;104:126-133.
38. Choi UH, Jung BM. Ion conduction, dielectric and mechanical properties of epoxy-based solid polymer electrolytes containing Succinonitrile. *Macromol Res*. 2018;26:459-465.
39. Smiglak M, Reichert WM, Holbrey JD, et al. Combustible ionic liquids by design: is laboratory safety another ionic liquid myth? *Chem Commun*. 2006;2554-2556.
40. Abdallah T, Lemordant D, Claude-Montigny B. Are room temperature ionic liquids able to improve the safety of supercapacitors organic electrolytes without degrading the performances? *J Power Sources*. 2012;201:353-359.
41. Cao Y, Mu T. Comprehensive investigation on the thermal stability of 66 ionic liquids by Thermogravimetric analysis. *Ind Eng Chem Res*. 2014;53:8651-8664.
42. Diallo A-O, Morgan AB, Len C, Marlair G. An innovative experimental approach aiming to understand and quantify the actual fire hazards of ionic liquids. *Energ Environ Sci*. 2013;6:699-710.
43. Abbott AP, Harris RC, Ryder KS. Application of hole theory to define ionic liquids by their transport properties. *J Phys Chem B*. 2007;111(18):4910-4913.
44. ISO 5660-1: 2002 (E). Reaction-to-fire tests e heat release, smokeproduction andmassloss rate. Part 1: heat release rate (cone calorimeter method). Geneva, Switzerland; 2002.
45. Hakkarainew T. *Smoke Gas Analysis by Fourier Transform Infrared Spectroscopy*. Espoo: VTT Technical Research Centre of Finland; 1999.
46. ISO 19702:2006. Toxicity testing of fire effluents — Guidance for analysis of gases and vapours in fire effluents using FTIR gas analysis; 2006.
47. Guillaume E, Saragoza L. In Application of FTIR analysers to fire gases – progress in apparatus and method validation for quantitative analysis. The 14th International Conference on Fire and Materials, San Francisco, CA, USA; 2015:2-4.
48. Pottel H. The use of partial least squares (PLS) in quantitative FTIR: determination of gas concentrations in smoke gases of burning textiles. *Fire Mater*. 1995;19(5):221-231.

49. Pottel H. Quantitative models for prediction of toxic component concentrations in smoke gases from FTIR spectra. *Fire Mater*. 1996;20(6):273-291.
50. Speitel L. *DOT FAA/AR-01/88 Fourier Transform Infrared Analysis of Combustion Gases*. New Jersey: US Department of Transportation; 2001.
51. Speitel L. Fourier transform infrared analysis of combustion gases. *J Fire Sci*. 2002;20:349-371.
52. Fardell P, Guillaume E. Sampling and measurement of toxic fire effluent. In: Stec A, Hull R, eds. *Fire Toxicity*; Cambridge: Woodhead Publishing; 2010:385-423.
53. Stec AA, Fardell P, Blomqvist P, Bustamante-Valencia L, Saragoza L, Guillaume E. Quantification of fire gases by FTIR: experimental characterisation of calibration systems. *Fire Safety J*. 2011;46(5):225-233.
54. Tu V, Asp LE, Shirshova N, Larsson F, Runesson K, Jänick R. Performance of bicontinuous structural electrolytes. *Multifunct Mater*. 2020;3:025001.
55. Ge R, Hardacre C, Nancarrow P, Rooney D. Thermal conductivities of ionic liquids over the temperature range from 293 K to 353 K. *J Chem Eng Data*. 2007;52:1819-1823.
56. Tomida D, Kenmochi S, Tsukada T, Yokoyama C. Measurements of thermal conductivity of 1-Butyl-3-methylimidazolium Tetrafluoroborate at high pressure heat transfer. *Asian Res*. 2007;36:361-372.
57. Zhou T, Wang X, Cheng P, Wang T, Xiong D, Wang X. Improving the thermal conductivity of epoxy resin by the addition of a mixture of graphite nanoplatelets and silicon carbide microparticles. *eXPRESS Poly Lett*. 2013;7:585-594.
58. Gautam KR, Seth D. Thermal conductivity of deep eutectic solvents. *J Therm Anal Calorimetry*. 2020;140:2633-2640.
59. Chancelier L, Diallo AO, Santini CC, et al. Targeting adequate thermal stability and fire safety in selecting ionic liquid-based electrolytes for energy storage. *Phys Chem Chem Phys*. 2014;16:1967-1976.
60. Fredlake CP, Crosthwaite JM, Hert DG, Aki SNVK, Brennecke JF. Thermophysical properties of Imidazolium-based ionic liquids. *J Chem Eng Data*. 2004;49:954-964.
61. Patela P, Hulla TR, Steca AA, Lyon RE. Influence of physical properties on polymer flammability in the cone calorimeter. *Polym Adv Technol*. 2011;22:1100-1107.
62. Francesco FD, Calisi N, Creatini M, Melai B, Salvoc P, Chiappe C. Water sorption by anhydrous ionic liquids. *Green Chem*. 2011;13:1712-1717.
63. Delgado-Mellado N, Larriba M, Navarro P, et al. Thermal stability of choline chloride deep eutectic solvents by TGA/FTIR-ATR analysis. *J Molec Liquids*. 2018;260:37-43.
64. Babrauskas V, Peacock RD. Heat release rate: the single most important variable in fire Hazard. *Fire Safety J*. 1992;19:255-272.
65. Chen X, Jiao C, Li S, Sun J. Flame retardant epoxy resins from bisphenol-A epoxy curedwith hyperbranched polyphosphate ester. *J Polym Res*. 2011;18:2229-2237.
66. Wichman IS. Material flammability, combustion, toxicity and fire hazard in transportation. *Prog Energ Combust Sci*. 2003;29:247-299.

SUPPORTING INFORMATION

Additional supporting information may be found online in the Supporting Information section at the end of this article.

How to cite this article: Shirshova N, Rogaume T, Najmi H, Poisson M. The combustion behavior of epoxy-based multifunctional electrolytes. *Fire and Materials*. 2021;1–13. https://doi.org/10.1002/fam.2967